Available online at www.sciencedirect.com
ScienceDirect
Building and Environment 42 (2007) 1544–1552
BUILDING AND ENVIRONMENT
www.elsevier.com/locate/buildenv

Modeling of a novel Trombe wall with PV cells

Ji Jie*, Yi Hua, He Wei, Pei Gang, Lu Jianping, Jiang Bin

Department of Thermal Science and Energy Engineering, University of Science and Technology of China, Hefei, China

Received 13 November 2005; received in revised form 5 December 2005; accepted 17 January 2006

Abstract

A novel Trombe wall with PV cells is presented in this paper. A two-dimensional model of PV glass panel and a model of the PV-Trombe wall system are established. The temperature distribution and electrical performance of the PV-Trombe wall system are also obtained. Results show that according to the measured weather data and the special simulation condition, the temperature difference between the elements with and without PV cell on the glass panel reaches a maximum value of 10.6 °C; the temperature difference between the room with and without PV-Trombe wall reaches a maximum value of 12.3 °C during 3 days; after 7 days' operation, the all-day temperature of the room with PV-Trombe wall retains at about 13.4 °C and an increase of 5.00% for the electrical efficiency can be achieved.

Keywords: PV-Trombe wall; Temperature distribution; Electrical performance; PV glass panel

1. Introduction

A conventional Trombe wall is a south-facing concrete or masonry wall, blackened and covered on the exterior by glazing. It has been widely used and has improved much in past decades due to advantages such as simple configuration, high efficiency, zero running cost and so on [1]. Nevertheless, one of the important factors, which have limited its spread and application, is its unaesthetic property caused by the blackened massive wall.

More than 80% of the solar energy irradiated on the surface of a photovoltaic (PV) cell is converted into thermal energy rather than electrical energy, thus the temperature of PV cells increases and results in a drop of efficiency of PV cells. With PV cells being affixed back of the glass panel, a novel Trombe wall with PV cells (PV-Trombe wall) is constructed. The thermal energy on the surface of PV cells is removed by the air flow between the glass panel and wall, so the temperature of PV cells decreases and the electrical efficiency increases. It not only generates electricity, but also provides space heating; meanwhile it brings more aesthetic value.

Much theoretical and experimental research has been focused on the heat transfer, dynamics and performance analysis of Trombe wall. Smolec and Thomas have done the theoretical calculation about the temperature distribution of Trombe wall by using a thermal network and compared it with the experimental data [2]. Chen et al. have investigated the air flow in Trombe wall and deduced that the air flow is the function of the height of the air duct [3]. Guohui Gan has carried out the numerical simulation for Trombe wall using CFD techniques and investigated the effect of the distance between the wall and glazing, wall height, glazing type and wall insulation on the thermal performance of Trombe wall [4].

In the research of PV walls, Brinkworth et al. have deduced that with a well designed ventilated PV-wall structure, the PV cell temperature can be reduced by 15 °C and the PV-module power output can be increased by 8.3% [5,6]. Yang Hongxing and Ji Jie have established the heat transfer model of the PV-wall structure, numerically investigated the heat gain of the PV-wall and compared it with the heat gain of the massive wall without PV module.

*Corresponding author. Tel.: +86 551 3601652; fax: +86 551 3601652.
E-mail address: jijie@ustc.edu.cn (J. Jie).

0360-1323/$ - see front matter © 2006 Elsevier Ltd. All rights reserved.
doi:10.1016/j.buildenv.2006.01.005

Nomenclature

A sectional area normal to X direction of the air duct, m^2
A_{glass} area of PV glass panel, m^2
A_{in}, A_{out} areas of the bottom and top vent, respectively, m^2
A_{PV} total area of PV cells, m^2
C_f friction factor along the air duct
C_{in}, C_{out} loss coefficients at the bottom and top vent, respectively
C_G specific heat of glass, J/kg K
C_P specific heat of air, J/kg K
C_w specific heat of wall, J/kg K
d duct hydraulic diameter, i.e. $d = 2(w + D)$, m
D depth of the air duct, m
D_w wall thickness, m
E electric power rate generated by PV cells, W/m^2
E_{total} daily electricity generation, kWh
g gravitational acceleration, $g = 9.80665\,m/s^2$
G total incident solar radiation on the vertical plane of the PV glass panel, W/m^2
G_{total} daily solar radiation, kWh
Gr_x local Grashof number
h_{co}, h_{ci} convective heat transfer coefficients on the outside and inside surface of the PV glass panel, respectively, $W/m^2\,K$
h_{nwo}, h_{nwi} convective heat transfer coefficients on the outside and inside surface of the normal wall, respectively, $W/m^2\,K$
h_{nrwo} radiant heat transfer coefficient on the outside surface of the normal wall, $W/m^2\,K$
h_{ro}, h_{ri} radiant heat transfer coefficients on the outside and inside surface of the PV glass panel, respectively, $W/m^2\,K$
h_{rwo} radiant heat transfer coefficient on the outside surface of the blackened massive wall, $W/m^2\,K$
h_{wo}, h_{wi} convective heat transfer coefficients on the outside and inside surface of the blackened massive wall, respectively, $W/m^2\,K$
L height of PV-Trombe wall, m
L_{room} depth of the room, m
$\dot{m}$ mass flow rate of the air flow vented from the top vent, kg/s
N_{ux} local Nusselt number
R_{Trombe} ratio of the Trombe wall area to the total southern wall area
T_{nwo}, T_{nwi} temperatures of the outside and inside surface of the normal wall, respectively, K
T_p, T_e, T_a temperatures of the PV glass panel, environmental air and air in the air duct, respectively, K
T_{wo}, T_{wi} temperatures of the outside and inside surface of the blackened massive wall, K
T_r indoor temperature along X direction, K
$\overline{T}_r$ average indoor temperature, K
V ambient wind speed, m/s
V_a velocity of air flow in the air duct, m/s
w width of the PV-Trombe wall, m
w_{room} width of the room, m
X, Y, Z calculation height, thickness and width, respectively, m

Greek symbols

α absorptivity of PV cell
α_a thermal diffusivity of air, m^2/s
α_{wall} absorptivity of the outside surface of the blackened massive wall
α_{nwall} absorptivity of the normal wall
β heat expansion coefficient, K^{-1}
τ transmissivity of glass
ρ density of air, kg/m^3
ρ_G density of glass, kg/m^3
ρ_w density of wall, kg/m^3
λ_a thermal conductivity of air, W/m K
λ_G thermal conductivity of glass, W/m K
λ_w thermal conductivity of wall, W/m K
ε ratio of PV cell coverage
$\varepsilon_i, \varepsilon_o, \varepsilon_{wo}, \varepsilon_e$ emissivities of the inside and outside of the PV glass panel, the outside surface of the blackened massive wall and the ambient, respectively
ν kinematic viscosity of air, m^2/s
ξ_1, ξ_2, ξ_3 emissivity factors
σ Stefan–Boltzman constant, $W/m^2\,K^4$
η daily electrical efficiency
η_0 electrical efficiency under standard conditions (1000 W/m^2, 25 °C)
η_{total} total electrical efficiency during 7 days

Results show that the heat gain of PV-wall structures can be significantly reduced in summer, so that the cooling load of the building is decreased [7]. Ji Jie and He Wei have theoretically and experimentally investigated the performance of PV Walls with and without an air duct. Results show that different integration modes have only a small effect on the annual power output, but have an obvious effect on the annual heat gain [8,9]. In the research above, only the temperature distribution in the vertical direction is considered and there is no systemic calculation of Trombe wall.

A novel Trombe structure with PV cells is presented in this paper, and a new two-dimensional model of PV glass panel and a model of the PV-Trombe wall system are established. The temperature distribution and PV cells' electrical performance are numerically calculated by coupling the PV-Trombe wall and indoor room as a closed system.

2. Theoretical models

The only difference between the normal Trombe wall and the novel Trombe wall is that the novel Trombe wall structure with PV cells changes the normal glass panel to PV glass panel, on which some PV cells are affixed back of the glass panel. In order to obtain solar radiation on the blackened massive wall, the PV cells are grid distributed, as shown in Fig. 1, where X, Y, Z represent the height, thickness and the width direction, respectively. The ratio of PV cell coverage is defined as

$$\varepsilon = \frac{A_{PV}}{A_{glass}}, \tag{1}$$

where A_{PV} is the total area of PV cells and A_{glass} is the area of PV glass panel (m^2).

2.1. Energy balance of PV glass panel

The PV cells laminated on the back of the glass panel are very thin, the adherence between the PV cells and the glass is very tight and the heat conduction is good, so it is assumed that the temperature of the PV glass panel along Y direction is uniform. However, because the absorptivity of PV cells is higher than glass, the temperatures of the elements with and without PV cell are not uniform, even have great difference. A temperature difference with a maximum value of 10 °C has been substantiated according to our initial test. Hence, the temperature distribution of the PV glass panel is considered to be a two-dimensional (along X and Z direction) heat transfer problem, and this is much different from the processing methods adopted by Refs. [2–9] in which only the temperature distribution along X direction is considered. In order to simplify the calculations, it is assumed that the temperature of every PV cell is uniform and base-center grids are plotted along the boundary of every PV cell. As shown in Fig. 2, the PV cell is so thin that its heat capacity can be neglected, considering the heat capacity of the PV glass panel and the solar radiation, the energy balance equation of the PV glass panel is established according to Ref. [7]

$$\rho_G c_G \frac{\partial T_P}{\partial t} = \frac{\partial}{\partial X}\left(\lambda_G \frac{\partial T_P}{\partial X}\right) + \frac{\partial}{\partial Z}\left(\lambda_G \frac{\partial T_P}{\partial Z}\right) + b. \tag{2}$$

It is discretized as

$$\frac{\rho_G c_G (T_p - T_p^0)}{\Delta t} = \left[\frac{\lambda_G}{\Delta X_U \cdot \Delta X}(T_U - T_P) + \frac{\lambda_G}{\Delta X_D \cdot \Delta X}(T_D - T_P)\right] + \left[\frac{\lambda_G}{\Delta Z_W \cdot \Delta Z}(T_W - T_P) + \frac{\lambda_G}{\Delta Z_E \cdot \Delta Z}(T_E - T_P)\right] + b, \tag{3}$$

where $b = S_c + S_p T_p$, and subscripts U, D, W, E stand for the up, down, west, east control volume, respectively.

Through the analysis of the heat transfer control volumes of the PV glass panel, as shown in Fig. 3, it yields

(1) For the elements with PV cell on the glass panel:

$$S_c = [\alpha\tau + (1-\tau)]G - E + h_{co}T_e + \xi_1 h_{ro}T_e + h_{ci}T_a + \xi_2 h_{ri}T_{wo},$$

$$S_P = -(h_{co} + \xi_1 h_{ro} + h_{ci} + \xi_2 h_{ri}).$$

(2) For the elements without PV cell on the glass panel:

$$S_c = G(1-\tau) + h_{co}T_e + \xi_1 h_{ro}T_e + h_{ci}T_a + \xi_2 h_{ri}T_{wo},$$

$$S_P = -(h_{co} + \xi_1 h_{ro} + h_{ci} + \xi_2 h_{ri}),$$

where ρ_G, C_G, λ_G are the density (kg/m^3), specific heat (J/kg K) and thermal conductivity (W/m K) of glass, respectively; α is the absorptivity of PV cell; τ is the transmissivity of glass; G is the total incident solar radiation on the vertical plane of the PV glass panel (W/m^2);

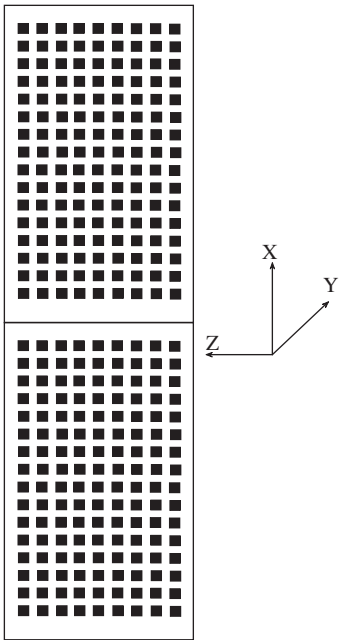

Fig. 1. Distribution scheme of PV cells on the glass panel.

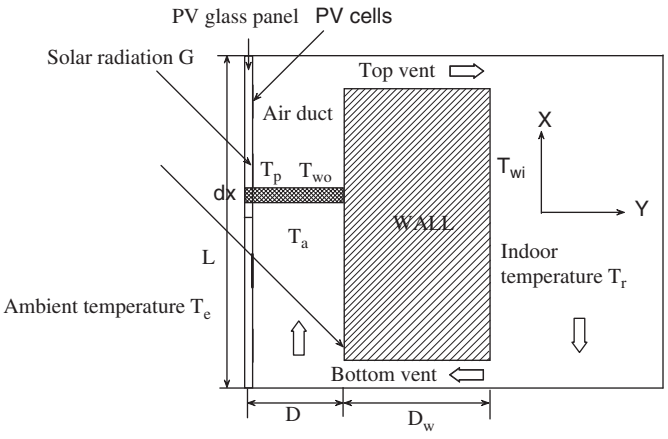

Fig. 2. Schematic diagram of a novel Trombe wall with PV cells.

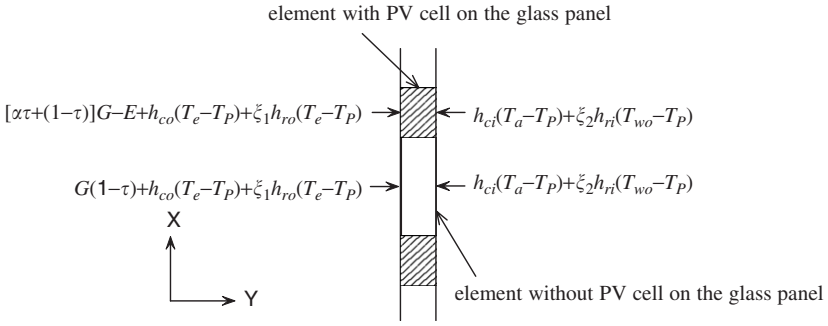

Fig. 3. Heat transfer control volumes of the PV glass panel (Y direction).

T_p, T_e, T_a and T_{wo} are the temperatures of the PV glass panel, environmental air, air in the air duct and the outside surface of the blackened massive wall, respectively, (K); ξ_1, ξ_2 are the emissivity factors on the outside and inside of the PV glass panel, respectively; h_{co}, h_{ci} are the convective heat transfer coefficients on the outside and inside surface of the PV glass panel, respectively, (W/m^2 K).

E is the electric power rate generated by PV cells (W/m^2) [10]

$$E = G \cdot \eta_0 \cdot [1 - 0.0045(T_p - 298.15)], \tag{4}$$

where η_0 is the electrical efficiency under standard conditions (1000 W/m^2, 25 °C), 14% is adopted in this paper.

h_{ro}, h_{ri} are the radiant heat transfer coefficients on the outside and inside surface of the PV glass panel, respectively, (W/m^2 K)

$$h_{ro} = \sigma(T_P^2 + T_e^2)(T_P + T_e), \tag{5}$$

$$h_{ri} = \sigma(T_P^2 + T_{wo}^2)(T_P + T_{wo}), \tag{6}$$

where σ is the Stefan–Boltzman constant, W/m^2 K^4.

The emissivity factors ξ_1, ξ_2 can be calculated from [11]:

$$\frac{1}{\xi_1} = \frac{1}{\varepsilon_o} + \frac{1}{\varepsilon_e} - 1, \tag{7}$$

$$\frac{1}{\xi_2} = \frac{1}{\varepsilon_i} + \frac{1}{\varepsilon_{wo}} - 1, \tag{8}$$

where $\varepsilon_i, \varepsilon_o, \varepsilon_{wo}, \varepsilon_e$ are the emissivities of the inside and outside of the PV glass panel, the outside surface of the blackened massive wall and the ambient, respectively.

2.2. Convective heat transfer coefficients

The convective heat transfer coefficient due to wind on the outside surface of the PV glass panel is given according to Ref. [11]

$$h_{co} = 5.7 + 3.8 \cdot V. \tag{9}$$

The convective heat transfer coefficient on the inside surface of the PV glass panel:

$$h_{ci} = \frac{N_{ux}\lambda_a}{X}, \tag{10}$$

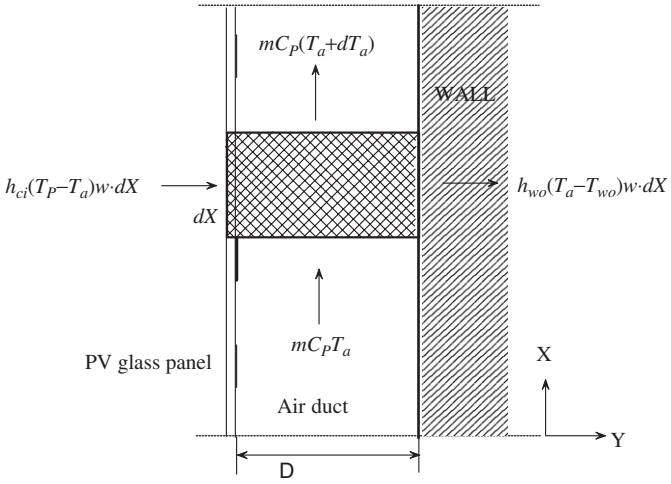

Fig. 4. Energy balance of the air control volume in the air duct.

where V is the ambient wind speed (m/s); λ_a is the thermal conductivity of air (W/m K); N_{ux} is the local Nusselt number.

According to Ref. [6]

$$N_{ux} = 0.12 \cdot (Gr_x \cdot \mathrm{Pr})^{1/3}, \tag{11}$$

$$Gr_x = g\beta \cdot (T_P - T_a) \cdot X^3/v^2, \quad \mathrm{Pr} = v/\alpha_a, \tag{12}$$

where v is the kinematic viscosity of air (m^2/s); α_a is the thermal diffusivity of air (m^2/s); g is the gravitational acceleration (m/s^2); β is the heat expansion coefficient (K^{-1}).

2.3. Energy balance in the air duct

The air per unit length in the air duct is taken as a control volume, as shown in Fig. 4. Though the PV glass panel consists of the PV part and glass part for a control volume, the temperatures of different parts are averaged along Z direction to simplify the calculations. Then it gives

$$\mathring{m}\, C_P T_a + h_{ci}(T_P - T_a)w \cdot dX = \mathring{m}\, C_P(T_a + dT_a) + h_{wo}(T_a - T_{wo})w \cdot dX + \rho C_P D \cdot w \cdot dX \frac{dT_a}{dt}, \tag{13}$$

where the mass flow rate of air $\mathring{m} = \rho w D \cdot V_a$, then it follows that

$$\rho D C_P \frac{dT_a}{dt} = h_{ci}(T_P - T_a) + h_{wo}(T_{wo} - T_a) - \rho V_a D C_P \frac{dT_a}{dX}, \quad (14)$$

where D is the depth of air duct (m); w is the width of the PV-Trombe wall (m); C_p is the specific heat of air (J/kg K); ρ is the density of air (kg/m^3), and V_a is the velocity of air flow in the air duct (m/s).

The velocity of air flow in the air duct V_a can be calculated as [7]

$$V_a = \sqrt{\frac{0.5 \times g\bar{\beta} \cdot (T_{out} - T_{in}) \cdot L}{C_f \frac{L}{d} + \frac{C_{in}A^2}{A_{in}^2} + \frac{C_{out}A^2}{A_{out}^2}}}, \quad (15)$$

where L is the height of PV-Trombe wall (m); d is the duct hydraulic diameter (m), i.e. $d = 2(w + D)$; A is the cross sectional area normal to X direction of the air duct (m^2), i.e. $A = w \times D$; A_{out}, A_{in} are the areas of the top and bottom vent, respectively, (m^2); C_f, C_{out}, C_{in} are the friction factor along the air duct, the loss coefficients at the top and bottom vent, respectively; $C_{out} = 0.3, C_{in} = 0.25, C_f = 0.3 \times 1.368 \times Gr_x^{0.084}$.

2.4. Heat transfer across the southern wall

The schematic of a comparable hot-box is shown in Fig. 5 where the southern wall consists of the blackened massive wall and the normal wall, and other walls consists of double insulated walls with an air interlayer between them for better insulation. For the blackened massive wall, considering the solar radiation transmitted through the elements without PV cell, the solar radiation on the outside surface per unit area of the blackened massive wall is $G \cdot \alpha_{wall} \cdot \tau \cdot (1 - \varepsilon)$, where α_{wall} is the absorptivity of the outside surface of the blackened massive wall.

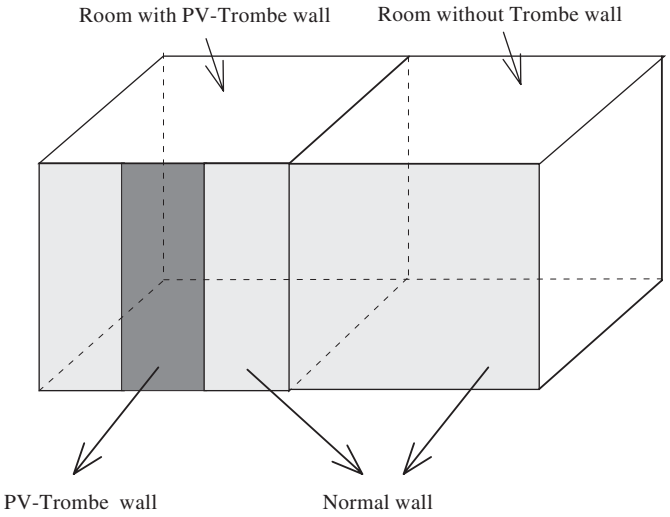

Fig. 5. Schematic of the comparable hot-box.

It is assumed that the heat transfer across the blackened massive wall is one-dimensional [5–9]. The unsteady heat conduction equation is [7]

$$\frac{\partial T}{\partial t} = \frac{\lambda_w}{\rho_w C_w} \frac{\partial^2 T}{\partial^2 Y},$$

$$-\lambda_w \left(\frac{\partial T}{\partial Y}\right)_{y=0} = h_{wo}(T_{wo} - T_a) + \xi_3 h_{rwo}(T_{wo} - T_p) + G\alpha_{wall}\tau(1 - \varepsilon), \quad (16)$$

$$-\lambda_w \left(\frac{\partial T}{\partial Y}\right)_{y=D_w} = h_{wi}(T_{wi} - \bar{T}_r),$$

$$T_{\tau=0} = T|_0(Y), \quad (17)$$

where $\rho_w, C_w, \lambda_w, D_w$ are the density (kg/m^3), specific heat (kg/m^3), thermal conductivity (W/m K) and thickness (m) of wall, respectively; T_{wi} is the temperature of the inside surface of the blackened massive wall (K); $\overline{T}_r$ is the average indoor temperature (K); h_{wo}, h_{wi} are the convective heat transfer coefficients on the outside and inside surface of the blackened massive wall (W/m^2 K), respectively; h_{rwo} is the radiant heat transfer coefficient on the outside surface of the blackened massive wall (W/m^2 K), $h_{rwo} = h_{ri}$. The emissivity factor $\xi_3 = \xi_2$.

For the normal wall, Eq. (16) is used for calculation and the relevant boundary conditions are as follows:

$$-\lambda_w \left(\frac{\partial T}{\partial Y}\right)_{y=0} = h_{nwo}(T_{nwo} - T_e) + \xi_1 h_{nrwo}(T_{nwo} - T_e) + G\alpha_{nwall},$$

$$-\lambda_w \left(\frac{\partial T}{\partial Y}\right)_{y=D_w} = h_{nwi}(T_{nwi} - \bar{T}_r),$$

where T_{nwo}, T_{nwi} are the temperatures of the outside and inside surface of the normal wall, respectively, (K); h_{nwo}, h_{nwi} are the convective heat transfer coefficients on the outside and inside surface of the normal wall, respectively, (W/m^2 K); h_{nrwo} is the radiant heat transfer coefficient on the outside surface of the normal wall, (W/m^2 K); α_{nwall} is the absorptivity of the normal wall.

2.5. Heat transfer in the room

In order to simplify the calculations, it is assumed that only the heat transfer across the southern wall is considered while the heat transfer across other walls is not considered in a hot-box room as a result of their favorable insulation, and the indoor temperature varies along X direction only. The energy balance equation in the room is obtained similarly

$$\mathring{m} C_P T_r + [(1 - R_{Trombe}) \cdot h_{nwi}(T_{nwi} - T_r) + R_{Trombe} \cdot h_{wi}(T_{wi} - T_r)] \cdot w_{room} \cdot dX = \mathring{m} C_P (T_r + dT_r) + \rho C_P L_{room} \cdot w_{room} \cdot dX \frac{dT_r}{dt} \quad (18)$$

it follows that

$$\rho C_P L_{\text{room}} \frac{\mathrm{d}T_r}{\mathrm{d}t} = R_{\text{Trombe}} \cdot h_{\text{wi}}(T_{\text{wi}} - T_r) + (1 - R_{\text{Trombe}}) \cdot h_{\text{nwi}}(T_{\text{nwi}} - T_r) - \frac{\mathring{m}\, C_P}{w_{\text{room}}} \cdot \frac{\mathrm{d}T_r}{\mathrm{d}X}, \quad (19)$$

where T_r is the indoor temperature along X direction (K); $w_{\text{room}}, L_{\text{room}}$ are the width of the room along Z direction, the depth of the room along Y direction, respectively (m); $\mathring{m}$ is the mass flow rate of the air flow vented from the top vent (kg/s); R_{Trombe} is the ratio of the Trombe wall area to the total southern wall area.

3. Numerical simulation

In order to investigate the thermal and electrical performance of the novel Trombe wall with PV cells, a numerical simulation program is written in FORTRAN by authors for the comparable hot-box in different cases (PV-Trombe wall system, normal Trombe wall system without PV cells, system without Trombe wall). The measured weather data of Hefei's winter, as shown in Fig. 6, is configured as a data input file of the program, then the temperature distribution and electrical performance are discussed. The following parameters were used:

1. the width of the PV-Trombe wall $w = 0.84\,\text{m}$; the height $L = 2.66\,\text{m}$;
2. the depth of the air duct $D = 0.13\,\text{m}$; the areas of top and bottom vent are both $0.04\,\text{m}^2$;
3. the density of air $\rho = 1.18\,\text{kg/m}^3$; the specific heat $C_P = 1000\,\text{J/kg K}$; the thermal conductivity $\lambda_a = 0.026\,\text{W/m K}$; the kinematic viscosity $v = 1.58 \times 10^{-5}\,\text{m}^2/\text{s}$;
4. the thickness of the wall (red brick structure) $D_w = 240\,\text{mm}$; the density $\rho_w = 1800\,\text{kg/m}^3$; the specific heat $C_w = 840\,\text{J/kg K}$; the thermal conductivity $\lambda_w = 0.814\,\text{W/m K}$;
5. the thickness of glass is 3 mm; the density $\rho_G = 2515\,\text{kg/m}^3$; the specific heat $C_G = 810\,\text{J/kg K}$; the thermal conductivity $\lambda_G = 1.4\,\text{W/m K}$; the transmissivity $\tau = 0.9$;
6. the ratio of PV cell coverage $\varepsilon = 0.324$; the absorptivity of PV modules $\alpha = 0.9$; the absorptivity of the blackened massive wall $\alpha_{\text{wall}} = 0.9$; the absorptivity of the normal wall $\alpha_{\text{nwall}} = 0.72$; the emissivities of the wall and glass panel surfaces are 0.9;
7. the size of the hot-box room: width $w_{\text{room}} = 3.00\,\text{m}$, depth $L_{\text{room}} = 3.00\,\text{m}$, height is 2.66 m.

Two PV glass panels are fixed on the frame. Both the top and bottom vent are opened at 10:00, closed at 16:00 everyday. The time step is 20 s and the initial time is 1:00. The initial indoor temperature is 2 °C according to the measured data.

Results are as shown below:

3.1. The temperature of the PV glass panel

Fig. 7 shows the temperatures on the PV glass panel. TC1, TC2 are the temperatures of the element with and without PV cell in the centre of the upper PV glass panel; TC3, TC4 are the temperatures of the element with and without PV cell in the centre of the lower PV glass panel. $\delta\text{TC} = (\text{TC1} - \text{TC2} + \text{TC3} - \text{TC4})/2$, δTC is the average temperature difference between the elements with and without PV cell, as shown in Fig. 8. From the two figures, the temperature of the upper PV glass panel is slightly higher than that of the lower one, for both the elements with and without PV cell. The average temperature difference between the elements with and without PV cell reaches a maximum value of 10.6 °C and its behavior follows the variation of solar radiation.

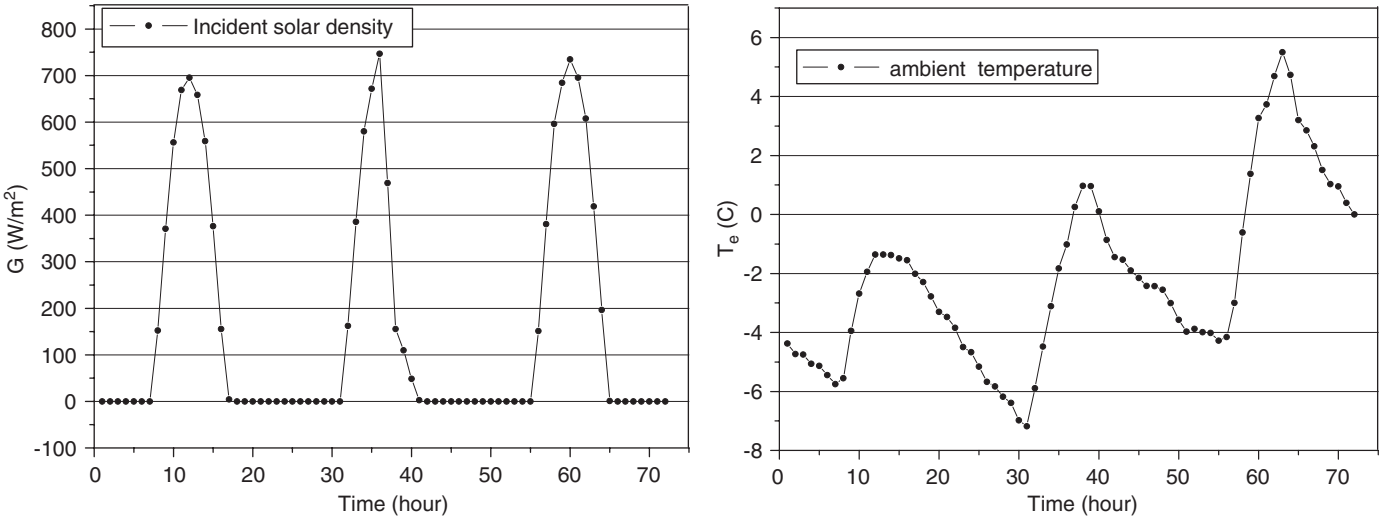

Fig. 6. Measured weather data of Hefei's winter.

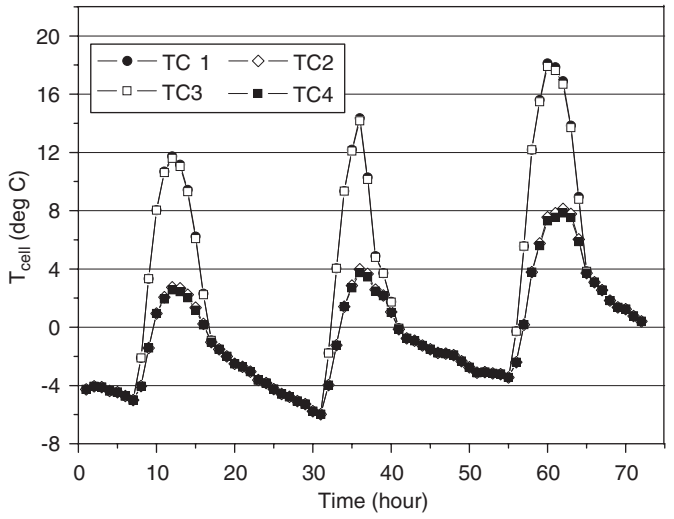

Fig. 7. Temperature distribution on the PV glass panel.

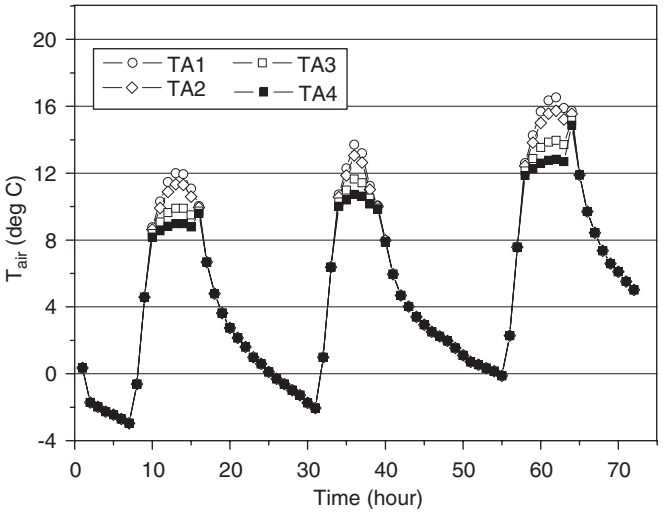

Fig. 9. Air temperature in the air duct.

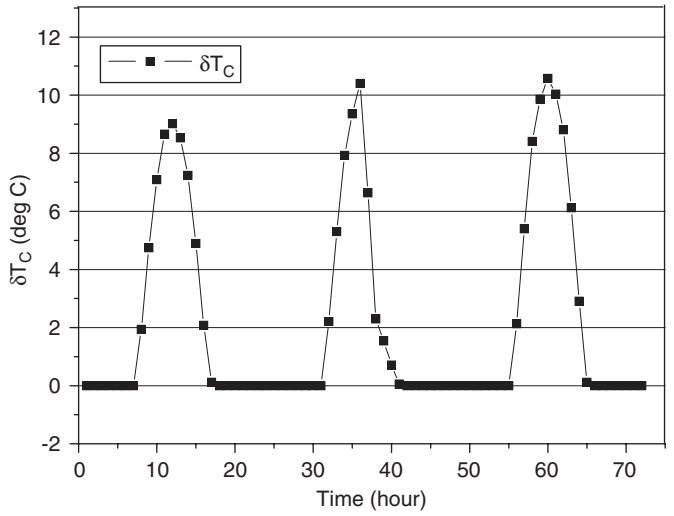

Fig. 8. The average temperature difference between the elements with and without PV cell on the glass panel.

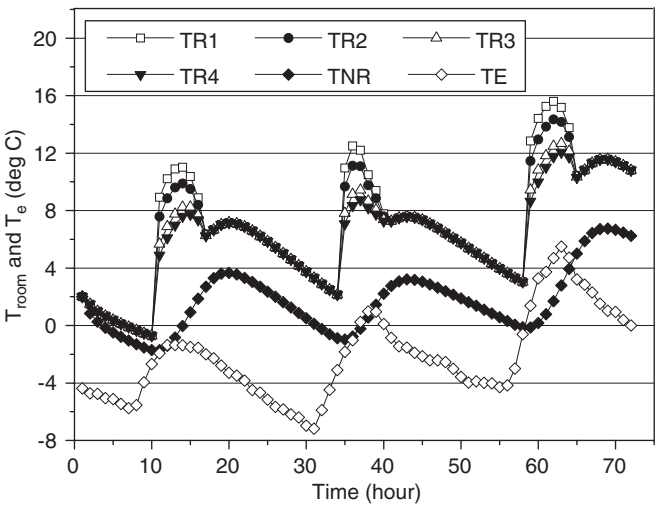

Fig. 10. Comparison of the temperatures in the room with and without PV-Trombe wall, and ambient temperature.

3.2. The temperature of the air in the air duct

Fig. 9 shows the air temperatures in the air duct. TA1, TA2, TA3, TA4 are the temperatures at the $\frac{4}{5}, \frac{3}{5}, \frac{2}{5}, \frac{1}{5}$ times of the height of the air duct, respectively. From Fig. 9, the temperature in the air duct increases with the increase of height. The acute part of TA3, TA4 in the figure is due to the saltation of the temperature when the top and bottom vent are closed at 16:00 everyday.

3.3. The temperature of the rooms

Fig. 10 shows the temperatures of the room with and without PV-Trombe wall, and ambient temperature. TR1, TR2, TR3, TR4 are the PV-Trombe wall indoor temperatures at the $\frac{4}{5}, \frac{3}{5}, \frac{2}{5}, \frac{1}{5}$ times of the height of the hot-box room, respectively. TNR is the indoor temperature of the system without Trombe wall, TE is the ambient temperature. Fig. 11 shows the temperature difference between the average temperature of the room with and without PV-Trombe wall. From Figs. 10 and 11, with the increase of height, the indoor temperature of the PV-Trombe wall system increases; the indoor temperature escalates during the first 3 days and the temperature difference between the two rooms reaches a maximum value of 12.3 °C. The first peak value of the daily indoor temperature of the PV-Trombe wall system is due to the solar radiation and the second is due to the thermal storage function of the blackened massive wall.

Fig. 12 shows the simulation results after 7 days' operation according to the repeating adoption of the third day's weather data in the latter 4 days. TR is the average temperature of the room with PV-Trombe wall. TR retains about 13.4 °C after 7 days' operation. By increasing the area of PV-Trombe wall or insulating the interior surface

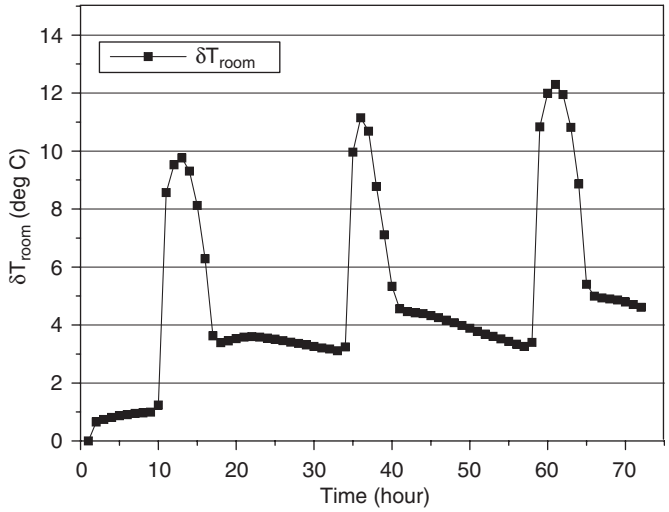

Fig. 11. The temperature difference between the room with and without PV-Trombe wall.

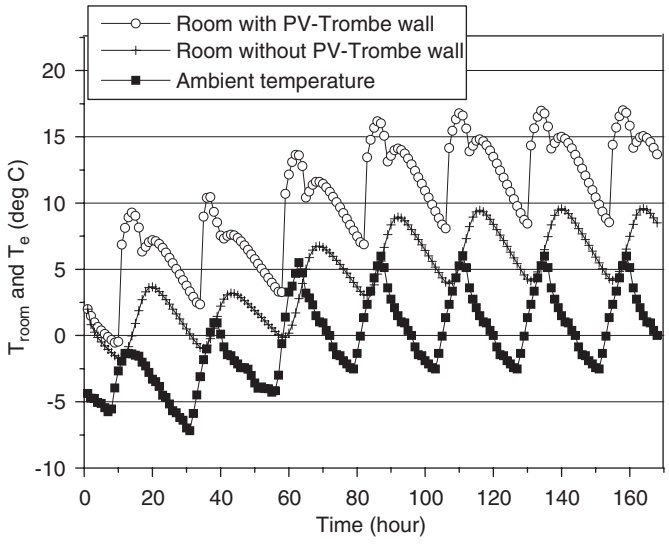

Fig. 12. Comparison of the temperatures in the room with and without PV-Trombe wall, and ambient temperature after 7 days' operation.

of the massive wall, the need of space heating will be satisfied.

Fig. 13 shows the indoor temperatures for different rooms (the room with PV-Trombe wall, with normal Trombe wall, without Trombe wall). From Fig. 13, the indoor temperature of the PV-Trombe wall system is lower compared with that of the normal Trombe wall system, because of the shading of solar radiation by PV cells. However, as a new type of BIPV/T (Building Integrated with Photovoltaic/Thermal), PV-Trombe wall system can provide space heating at the same time while generating electrical energy, and the aesthetic value is much more than that of normal Trombe wall so that it will have more application prospects.

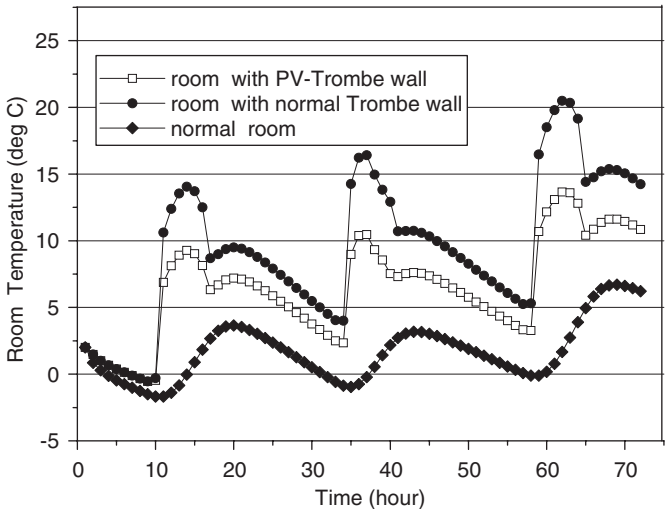

Fig. 13. The indoor temperatures for different rooms.

Table 1
Daily solar radiation, electricity generation, electric efficiency after 7 days' operation

Day	G_{total} (kWh)	E_{total} (kWh)	$\eta = E_{total}/(G_{total} \cdot \varepsilon)$
1	9.3356	0.4548	0.1504
2	7.4100	0.3598	0.1499
3	9.9333	0.4726	0.1468
4	9.9333	0.4691	0.1458
5	9.9333	0.4690	0.1457
6	9.9333	0.4690	0.1457
7	9.9333	0.4690	0.1457

3.4. The electrical performance

Table 1 shows the measured daily solar radiation (G_{total}), the calculated daily electricity generation (E_{total}) and electrical efficiency $\eta = E_{total}/(G_{total} \cdot \varepsilon)$ of the PV-Trombe wall system after 7 days' operation. The total electrical efficiency during 7 days $\eta_{total} = \sum E_{total}/(\sum G_{total} \cdot \varepsilon)$ is 0.1470, which increases by 5.00% compared to η_0 (14%), because the temperatures of the PV cells remain less than 20 °C when operating in winter (as shown in Fig. 7).

4. Conclusions

In the case of PV cells' grid-distribution on PV glass panel, the two-dimensional model of PV glass panel has been established. The simulation for PV-Trombe wall system has been conducted under the special simulation condition by using the measured weather data of Hefei's winter, and results have been compared with those of the system with normal Trombe wall and without Trombe wall. The comparative study gives the following results:

(1) The temperature difference between the elements with and without PV cell on the PV glass panel reaches a

maximum value of 10.6 °C during 3 days, so it is deduced that the two-dimensional model of PV glass panel is feasible.

(2) The temperature difference between the room with and without PV-Trombe wall reaches a maximum value of 12.3 °C during 3 days and the average indoor temperature retains about 13.4 °C after 7 days' operation. The indoor temperature of PV-Trombe wall system is lower compared with that of normal Trombe wall system, but the PV-Trombe wall system can provide space heating at the same time while generating electrical energy, and the aesthetic value is much more than that of normal Trombe wall.

(3) An increase of 5.00% for the electrical efficiency can be achieved with an air duct behind the PV modules.

(4) The computation program can be easily used in predicting the temperature distribution of a Trombe wall system at any time if the weather data of a certain zone and the relevant property parameters have been given. It is beneficial for the Trombe wall design and the analysis of its thermal performance.

Acknowledgements

The study was sponsored by National Science Foundation of China (NSFC). Project Number: 50408009.

References

[1] Yakubu GS. The reality of living in passive solar homes: a user experience study. Renewable energy 1996;8:177–81.
[2] Smolec W, Thomas A. Some aspects of Trombe wall heat transfer models. Energy Conversion Management 1991;32(3):269–77.
[3] Chen DT, Chaturvedi SK, Mohieldin TO. An approximate method for calculating laminar natural convective motion in a Trombe-wall channel. Energy 1994;19(2):259–68.
[4] Guohui Gan. A parametric study of Trombe walls for passive cooling of buildings. Energy and buildings 1998;27(1):37–43.
[5] Brinkworth BJ, Cross BM, Marshall RH, Hongxing Yang. Thermal regulation of photovoltaic cladding. Solar Energy 1997;61(3):169–78.
[6] Yang HX, Marshall RH, Brinkworth BJ. Validated simulation for thermal regulation of photovoltaic wall structures, Proceedings of the 25th photovoltaic specialist conference, USA, 1996.
[7] Yang Hongxing, Ji Jie. Study on the heat gain of a PV-wall. Taiyangneng Xuebao/Acta Energiae Solaris Sinica 1999;20(3):270–3.
[8] Ji Jie, He Wei. Dynamic prediction of the annual heat gain and power output of a PV-wall. Taiyangneng Xuebao/Acta Energiae Solaris Sinica 2001;22(3):311–6.
[9] Ji Jie, He Wei. The theoretical and experimental research on the performance of PV-wall with different modes of natural cooling. Taiyangneng Xuebao/Acta Energiae Solaris Sinica 2001;22(4):380–4.
[10] Zondag HA, De Vries DW, Van Helden WGJ, Van Zolingen RJC, Van Steenhoven AA. The thermal and electrical yield of a PV-thermal collector. Solar Energy 2002;72(2):113–28.
[11] Duffie JA, Beckman WA. Solar engineering of thermal processes. 2nd ed. New York: Wiley; 1991.